I-1. PROJECT RESEARCHES

Project 10

PR10 Solution Chemical Studies on Actinides and Fission Product Nuclides

A. Uehara

National Institute for Quantum and Radiological Science and Technology

OBJECTIVE:

Chemistry of actinide and fission product nuclides in various kinds of solutions such as aqueous, organic solutions including ionic liquids plays important role on the nuclear fuel cycle and radioactive waste disposal. The ionic species of the actinide and fission products dissolving into the solutions are strongly affected by the various kinds of parameter, concentration of H^+, electrolyte, oxygen, organic/inorganic ligands, and so on. Hot laboratory of KUR is one of core facilities in which various nuclides can be handles. Here, these nuclides can be obtained by the irradiation in the reactor core. Collaboration researches have been progressed with the field of nuclear science as well as material, environmental sciences after the accident in Fukushima Dai-ichi Nuclear Power Plant. The following research subjects have been studied to enhance an activation on science of actinide and fission product nuclides as well as the use of hot laboratory:

P10-1 Kinetic and equilibrium analysis of actinide and FP elements in molten salts (T. Goto, *et al.*)

P10-2 Study on complexation behavior of actinide and FP elements in radioactive waste disposal environment (T. Kobayashi, *et al.*)

P10-3 Study on the redox behavior of uranium and FP elements in molten chloride (Y. Sakamura, *et al.*)

P10-4 Study on dissolution behavior of actinide and FP elements in fuel debris (T. Sasaki, *et al.*)

P10-5 Application of isotope ratio analysis to radio nuclide analysis in environmental samples (Y. Shibahara, *et al.*)

P10-6 Activity measurement of dissolved chemical species in molten salt using halide ion conductor (H. Sekimoto, *et al.*)

P10-7 Effects of neutron irradiation and uranium addi tion on borosilicate glass structure (T. Nagai, *et al.*)

P10-8 Neutron cross section studies of actinides and fission nuclides (S. Nakamura, *et al.*)

P10-9 Interaction of inorganic compounds with trit ium ion in aqueous solution (H. Hashizume, *et al.*)

P10-10 Solvent extraction studies of uranium and fission product elements (T. Fujii, *et al.*)

P10-11 Electrochemical and spectroscopic studies for dry recycling process development (Matsuura, *et al.*)

RESULTS:

Some groups reported the environmental analyses and separation of radio nuclides produced by Fukushima Dai-ichi Nulcear Power Plant. Sasaki, *et al.* studied the preparation of the molten core-concrete interaction (MCCI) debris using a mixture of uranium and zirconium oxides, and a component of cement material such as calcium which is simulated to the bottom of the primary containment vessel. The simulated MCCI debris was irradiated at KUR to produce radionuclides. Shibahara, *et al.* reported the applicability of the thermal ionization mass spectrometry (TIMS) for the analysis of cesium Cs isotopes released on the accident of Fukushima Dai-ichi Nuclear Power Plant. Matsuura, *et al.* proposed selective fluorination using HF to dissolve into molten salt and electrodeposition uranium as a metal or oxides at the electrode in the molten salts. Hashizume, *et al.* studied the change of the ion exchange between tritium in water and proton in a hydroxide to the different concentration of tritium in water, and showed the isotherm for the ion exchange between tritium and proton to the concentration of tritium in water by the hydroxide.

Chemical separation of radioactive elements has been extensively applied in nuclear science fields because there are long-term options for management of spent nuclear fuels: storage for nuclear wastes in a deep geological repository and separation and recycling of the actinide elements. Nagai, *et al.* reported that the structural change of borosilicate glass dissolving simulated high-level radioactive elements was observed by Raman spectroscopy after neutron irradiation at KUR. Fujii, *et al.* focused on the separation of palladium and studied the solvent extraction behavior of palladium from a nitric acid solution using newly prepared organic ligands. Sakamura, *et al.* reported that redox behavior of selenium and tellurium ions in molten lithium-potassium chloride melts were investigated by in-situ uv-vis absorption spectroscopy for developing pyrochemical reprocessing of spent oxide fuels. A new type reference electrode in molten chlorides consisted of silver, pure silver chloride and anion conducting solid electrolyte such as calcium oxide doped lanthanum oxychloride was proposed by Sekimoto, *et al.* The thermal-neutron cross-section of the ^{135}Cs $(n,\gamma)^{136}Cs$ reaction was measured by Nakamura, *et al.* to evaluate the transmutation and reaction rate. For the safety assessment of radioactive waste disposal, it is necessary to predict the solubility limit of radionuclides under relevant repository conditions. Kobayashi, *et al.* investigated the uranium(VI) solubility in the presence of isosaccharinic acid (ISA), which is known as one of the main degradation products, dominant U(VI)-ISA complex was revealed, and the formation constant was determined by the analysis of the solubility data.

ACKNOWLEDGEMENTS:

This project was supported by Profs. Ohtsuki, Takamiya, and Sekimoto in KURNS.

PR10-1 Solubility of U(VI) in the presence of isosaccharinic acid

T. Kobayashi, D. Matoba, T. Fushimi, K. Haruki, T. Sasaki, T. Saito[1]

Graduate School of Engineering, Kyoto University
[1]Institute for Integrated Radiation and Nuclear Science, Kyoto University

INTRODUCTION: For the safety assessment of radioactive waste disposal, it is necessary to predict the solubility limit of radionuclides under relevant repository conditions. Cellulosic material contained in low and intermediate level waste degrades to smaller organic substances and α-isosaccharinic acid (ISA) is known as one of the main degradation products. ISA is a poly-hydroxycarboxylic acid and potentially enhance the solubility of radionuclides. Although several literatures have investigated the interaction of ISA with radionuclides, uranium is one of the elements, on which only very few studies have proposed the dominant ISA complexes and their formation constants [1]. Hexavalent uranium (U(VI)) is relevant under an occasional oxidizing condition in the repository system. Rao et al. has determined the complex formation constants of $UO_2(ISA)^{2+}$, $UO_2(ISA)_2(aq)$ and $UO_2(ISA)_3^-$ based on the potentiometric and calorimetric measurements [2]. In their experiments, the pH range was limited to the acidic pH region and thus U(VI)-ISA species dominant in neutral to alkaline pH range is still unclear. Since the U(VI) solubility in neutral to alkaline pH region is controlled by sparingly soluble $Na_2U_2O_7{\cdot}H_2O$(cr), formation of stable U(VI)-ISA species increases the uranium solubility in the repository system. In the present study, we investigated the U(VI) solubility in the presence of ISA at hydrogen ion concentrations (pH_c) of 7–13 and total concentration of ISA ($[ISA]_{tot}$) of 10^{-4} to $10^{-1.2}$ mol/dm^3 (M). Based on the slope analysis of the solubilities, dominant U(VI)-ISA complex was revealed, and the formation constant was determined by the analysis of the solubility data.

EXPERIMENTS: A stock solution of 0.33 M U(VI) was prepared by dissolving $UO_2(NO_3)_2{\cdot}6H_2O$ in 0.1 M HNO_3. Portions of concentrated NaOH solution was then quickly added into the U(VI) stock solution to obtain $Na_2U_2O_7{\cdot}H_2O$(cr) solid phase at pH_c about 10. Calcium isosaccharinate ($Ca(ISA)_2$) was synthesized from α-lactose and converted to NaISA stock solution. Sample solutions at specific pH_c and $[ISA]_{tot}$ were prepared by an undersaturation method. Before adding the $Na_2U_2O_7{\cdot}H_2O$(cr) to each sample tube, pH_c and $[ISA]_{tot}$ were adjusted in the ranges of pH_c = 7–13 and $[ISA]_{tot}$ = 10^{-4} to $10^{-1.2}$ M by adding appropriate amount of HCl/NaOH and NaISA stock solution. The ionic strength of each sample solution was set to I = 0.5 using 5 M NaCl stock solution. The sample tubes were kept in the Ar glove box up to maximum 123 days. After aging at a given period, the pH_c of the sample solutions was measured and each 0.5 mL of the supernatant was filtrated through ultrafiltration membrane (NMWL) of 10 kDa. The filtrate was acidified with nitric acid and diluted in 0.1 M HNO_3 for the measurement by ICP-MS. The detection limit was about 10^{-8} M.

RESULTS: U(VI) solubility in the absence and presence of $10^{-2.4}$ and $10^{-1.5}$ M ISA was investigated as a function of pH_c. In the absence of ISA, the solubility plots obtained in the present study are in good agreement with the literature values reported as the solubility of $Na_2U_2O_7{\cdot}H_2O$(cr) [3,4]. In the presence of $10^{-2.4}$ and $10^{-1.5}$ M ISA, the solubility was higher than those in the absence of ISA and almost constant against pH_c. Provided that the solid phase is $Na_2U_2O_7{\cdot}H_2O$(cr), the slope of zero suggested that three OH^- ions were involved in the U(VI)-ISA complex. At fixed pH_c 8.4 and 10.5, the U(VI) solubility was investigated as a function of total ISA concentrations ($[ISA]_{tot}$). U(VI) solubility increased with an increase of $[ISA]_{tot}$ with a slope of approximately 2, indicating that two ISA ligands were involved in the U(VI)-ISA complex. In conjunction with the slope of U(VI) solubility against pH_c and $[ISA]_{tot}$, the dominant U(VI)-ISA species was found to be $UO_2(OH)_3(ISA)_2^{3-}$ with the formation reaction of $UO_2^{2+} + 3OH^- + ISA^- \rightleftharpoons UO_2(OH)_3(ISA)_2^{3-}$. Taking the complex formation constant (β_{132}) of $UO_2(OH)_3(ISA)_2^{3-}$, hydrolysis constants of U(VI) (β_{1m}) [1], and solubility product of $Na_2U_2O_7{\cdot}H_2O$(cr) (K_{sp}) [4] into account, U(VI) solubility ([U(VI)]) can be described as

$$[U(VI)] = [UO_2^{2+}] + \sum_{m,n}[(UO_2^{2+})_m(OH)_n^{2m-n}] + [(UO_2^{2+})(OH)_3(ISA)_2^{3-}]$$

The solubility data in the neutral to alkaline pH range were analyzed to determine the complex formation constants β_{132} in the least squares fitting analysis. The formation constant was determined to be $\log \beta_{132} = 27.5 \pm 0.1$. The increase of the U(VI) solubility in the presence of ISA was quantitatively well explained by the formation of $UO_2(OH)_3(ISA)_2^{3-}$.

REFERENCES:

[1] Hummel W *et al.,* Chemical Thermodynamics of Compounds and Complexes of U, Np, Pu, Am, Tc, Se, Ni and Zr with Selected Organic Ligands. Elsevier, North-Holland, Amsterdam (2005).
[2] Rao L *et al.*, Radiochim. Acta, **92** (2004) 575-581.
Baes C. F., Mesmer R. E. The Hydrolysis of Cations. John Wiley & Sons, New York (1976).
[3] Yamamura T *et al.,* Radiochim. Acta, **83** (1998) 139-146.
[4] Altmaier M *et al.,* J. Chem. Thermodynamics **114** (2017) 2–13.

PR10-2 Electronic Absorption Spectra of Sulfer in LiCl-KCl Eutectic Melt

Y. Sakamura[1], T. Murakami[1], K. Uozumi[1] and A. Uehara[2]

[1]Central Research Institute of Electric Power Industry
[2]National Institutes for Quantum and Radiological Science and Technology

INTRODUCTION: The electrolytic reduction technique in LiCl-Li_2O melts has been developed for pyrochemical reprocessing of spent oxide fuels. At the cathode, actinide oxides are reduced to their metals:

$$MO_2 + 4\ e^- \rightarrow M + 2\ O^{2-} \qquad (1)$$

where M denotes actinides such as U and Pu. Similar to oxygen, chalcogen fission products such as Se and Te are dissolved into the melt in the form of divalent anion.

Recently, the authors have studied electrochemical behaviors of Na_2Se and Na_2Te in LiCl-KCl eutectic melt to extract Se and Te from molten salts [1]. It was indicated that the deposition of Te proceeded in two steps at the anode: the oxidation of Te^{2-} to Te_2^{2-} occurred followed by the oxidation of Te_2^{2-} to Te, which was similar to the electrochemical behaviors of Se and S [2]. Moreover, the absorption spectra of Na_2Se and Na_2Te in LiCl-KCl melt have been already reported [3,4]. In this study, Li_2S was investigated to compare the spectroscopic characteristics among S^{2-}, Se^{2-} and Te^{2-}.

EXPERIMENTS: LiCl-KCl-Li_2S (Li_2S: 0.44 wt%) and LiCl-KCl-Li_2S-S (Li_2S: 0.48 wt%, S: 1.5 wt%) mixtures were prepared by heating quartz tubes containing LiCl-KCl eutectic (59:41 mole ratio), Li_2S (99.9% purity) and S (99.999% purity) at temperatures > 673 K.

LiCl-KCl-Li_2S test

LiCl-KCl eutectic (4.079 g) was loaded in a rectangular quartz cell (10 x 10 mm) used for absorption spectrometry and heated to 673 K in an electric furnace. The experimental apparatus was previously described in detail by Nagai et al. [5] The LiCl-KCl-Li_2S mixture (0.211 g) was then added and the absorption spectrum of the melt was measured by using an UV/Vis/NIR spectropho-tometer (V-570, JASCO).

LiCl-KCl-Li_2S-S test

LiCl-KCl eutectic (4.013 g) was loaded in a rectangular quartz cell and heated to 673 K. The LiCl-KCl-Li_2S-S mixture (0.086 g) was then added and the absorption spectrum of the melt was measured. Subsequently, S (0.012 g) was added.

All of the experiments were conducted in a high-purity argon atmosphere glove box.

RESULTS: Fig. 1 shows absorption spectra of the melts. No peak was present in the wavelength range of 1000-2000 nm. The absorption peak at 333 nm (Fig. 1, (a)) increased as the LiCl-KCl-Li_2S mixture was added, which has not been reported before. The LiCl-KCl-Li_2S-S melt was light blue and there was an absorption peak at 580 nm (Fig. 1, (b)). The cyclic voltammetric studies in LiCl-KCl-Li_2S melts showed that S is deposited on inert anodes such as Au via intermediate products of polysulfide ions (S_n^{2-}) [2]:

$$S^{2-} \rightarrow S_n^{2-} \rightarrow S_n \qquad (2)$$

Therefore, it is suggested that the absorption peak at 580 nm might be due to the S_n^{2-} ions, which is consistent with the results previously measured in a LiCl-KCl melt after the cathodic dissolution of liquid S [6]. The subsequent addition of S into the melt led to a large increase in the peak height (Fig. 1, (c)), and the melt became dark blue. The peak wavelength remained at 580 nm, indicating that the addition of S might not change the polysulfide species. After the measurement, evaporated S was found on the upper part of quartz cell. The mass balance of S in the melt should be examined in detail in future work.

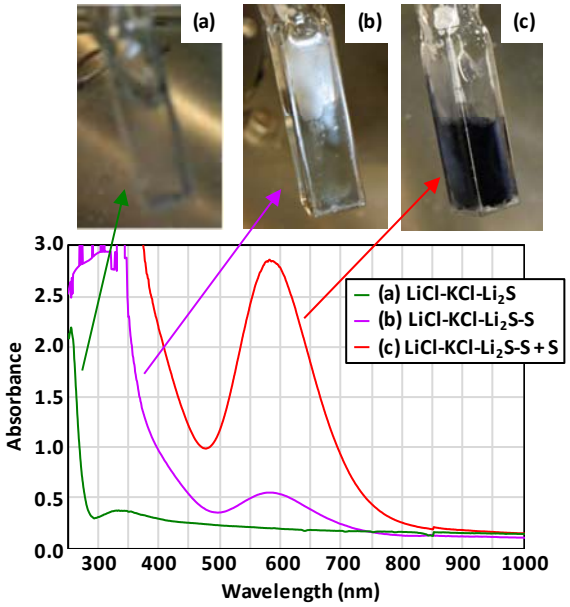

Fig. 1 Absorption spectra of (a) "LiCl-KCl-Li_2S", (b) "LiCl-KCl-Li_2S-S" and (c) "LiCl-KCl-Li_2S-S +S" melts.

ACKNOWLEDGMENTS: The authors are grateful to Drs. K. Takamiya and T. Ohtsuki of Institute for Integrated Radiation and Nuclear Science, Kyoto University, for their support and useful advice.

REFERENCES:

[1] Y. Sakamura, T. Murakami and K. Uozumi, Proc. The 49th Symposium on Molten Salt Chemistry, p. 84, Kansai Univ., Japan, Nov. 30 - Dec. 1, 2017, in Japanese.
[2] D. Warin, Z. Tomczuk and D.R. Vissers, J. Electro-chem. Soc., 130 (1983) 64-70.
[3] Y. Sakamura, T. Murakami, K. Uozumi, A. Uehara and T. Fujii, KURRI Progress Report 2016 (2017) 15.
[4] Y. Sakamura, T. Murakami, K. Uozumi, A. Uehara and T. Fujii, KURRI Progress Report 2017 (2018) 192.
[5] T. Nagai, T. Fujii, O. Shirai and H. Yamana, J. Nucl. Sci. Technol., 41 (2004) 690-695.
[6] F.G. Bodewig and J.A. Plambeck, J. Electrochem. Soc., 117 (1970) 904.

PR10-3 Study on the leaching behavior of fission products in simulated MCCI debris

T. Sasaki, N. Sato[1], A. Kirishima[1], D. Akiyama[1], T. Kobayashi, K. Takamiya[2], S. Sekimoto[2], S. Sakamoto and Y. Kodama

Graduate School of Engineering, Kyoto University

[1] Institute of Multidisciplinary Research for Advanced Materials, Tohoku University

[2] Institute for Integrated Radiation and Nuclear Science, Kyoto University

INTRODUCTION: Information on the radionuclide behavior in fuel debris and surface seawater will be helpful to analyze the forthcoming analysis data about the contents of minor FPs and TRU in the contaminated water, and to manage associated secondary wastes. A molten core-concrete interaction (MCCI) is thought to be a critical event because of the penetration of partially molten core from the reactor pressure vessel to the bottom of the primary containment vessel. The physical and chemical characteristics of the MCCI debris have been studied using the knowledge obtained from similar events in other countries, and by using some calculation codes. Based on these fundamental findings, the initial composition of the debris, high-temperature and atmospheric conditions, and the cooling rate of molten core-concrete have a large impact on the solidification phases. However, the leaching behavior of fission products in MCCI debris has not been fully understood [1]. In the present study, the preparation of the MCCI debris are investigated using a mixture of UO_2, ZrO_2, and a component of cement material.

EXPERIMENTS: The reference cement material 211S was purchased from Japan Cement Association, and used without any preconditioning. Three cement mixing ratios of UO_2–ZrO_2 were adopted to obtain U:Ca mole ratios of 1:0.75 (#OA), 1:1.75 (#OB), and 1:6.75 (#OC). The mole ratio of U:Zr in UO_2–ZrO_2 sample was assumed to be 5:1, as a balance of UO_2 fuel and zircaloy clad. The weighed amounts of UO_2 and ZrO_2 powders and of the cement were mixed using an agate mortar and pestle. The sample was heated in a quartz boat at 1473 K for 2 h in an oxidizing (Ar + 2% O_2) atmosphere. During furnace cooling, pure argon gas was kept flowing. After the cooling, the sample was investigated by XRD. The simulated MCCI debris sealed in a quartz ampoule was inserted into a polyethylene capsule and irradiated using Pn-2 of Kyoto University Reactor (at 1 MW) for 20 min. The gamma-ray activity, which is considered as an initial inventory of each radionuclide in the solid sample, was measured using a Ge detector after cooling in order to allow for the decay of highly radioactive, short-lived nuclides.

RESULTS: The peaks of UO_2 phase in the mixed samples with ZrO_2 and CaO shifted to higher angles, which indicates the formation of a solid solution, $(Ca_yZr_zU_{1-y-z})O_{2+x}$ in #OA. The lattice parameter was 5.339 Å. It is recognized that the lattice parameters of the cubic-fluorite-type solid solution $(Ca_yZr_zU_{1-y-z})O_{2+x}$ changes with the stoichiometric abundances of metals and the O/M ratio. With increasing the Ca (and Si) amount to U, the dominant species changed from $(Ca_yZr_zU_{1-y-z})O_{2+x}$ in #OA (U:Ca = 1:0.75) to the trigonal $CaUO_4$ in #OB (U:Ca = 1:1.75), and Ca_3UO_6 in #OC (U:Ca = 1:6.75) appeared in the presence of further excess calcium. The nuclides were produced by the fission reaction of uranium-235. The peaks for five radionuclides—Zr-95, Ru-103, I-131, Cs-137, and Ba-140—were assigned in γ spectrometry. Zr-95 was produced from the fission reaction of uranium and the (n,γ) reaction of natural Zr-94 in the ZrO_2 matrix, suggesting that Zr-95 from two different origins exists in samples.

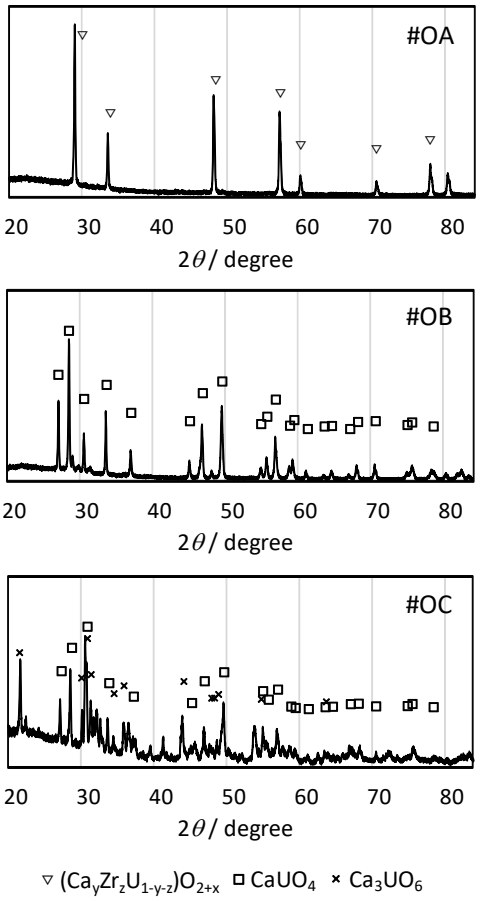

Fig. 1 XRD patterns of samples by heat treatment at 1473 K under O_2 atmospheric condition.

REFERENCES:

[1] Sasaki T., Takeno Y., Kirishima A., Sato N., J. Nucl. Sci. Technol., **53** (2016) 303–311.

PR10-4 **Analysis of isotopic composition of Cs recovered from environmental sample obtained in Fukushima prefecture by thermal ionization mass spectrometry**

Y. Shibahara, S. Fukutani, T. Kubota,
T. Shibata[1], M. Yoshikawa[1]

KURNS, Kyoto University
[1]Graduate School of Science, Hiroshima University

INTRODUCTION: We have studied the applicability of the mass spectrometry, especially thermal ionization mass spectrometry (TIMS), for the analysis of radionuclide released on the accident of Fukushima Dai-ichi Nuclear Power Plant. In the previous study of the analysis of Cs isotopic composition by TIMS, we compared the analytical result of isotopic composition of Cs in the standard materials and so on with the literature data to discuss the applicability of the isotopic analysis of Cs [1]. In this study, we discussed the analytical results of Cs isotopic composition obtained within the latest 2 financial years from April 2017 to March 2019.

EXPERIMENTS: Cs was recovered from the environmental sample of moss obtained in Fukushima prefecture. The concentration of ^{137}Cs of the environmental sample obtained in Fukushima prefecture was about 2.6×10^{-10} g/g (corrected on 11 Mar 2011). Cs was recovered according to the recovery scheme [2-4]. After the preparation of the samples for the isotopic composition analysis of Cs, the Cs isotopic ratios (= ^{134}Cs/^{137}Cs and ^{135}Cs/^{137}Cs) were analyzed by TIMS.

A thermal ionization mass spectrometer (TRITON-T1, Thermo Fisher Scientific) with a rhenium single filament system was used for the isotopic composition analysis of Cs. The Cs sample prepared for the TIMS analysis was loaded onto a rhenium filament with a TaO activator [2-4] or glucose activator [5]. Because of the loading amount of Cs (max. 1×10^{-12} g), the mass spectrometry was conducted with a secondary electron multiplier detector and the peak jump method [2-4].

RESULTS: The mass spectrum of Cs recovered from the environmental sample of moss was shown in Fig. 1. We can see the peaks corresponding to ^{134}Cs, ^{135}Cs and ^{137}Cs, aside from the peak of ^{133}Cs. Figure 2 shows the time profile of ^{134}Cs/^{137}Cs isotopic ratio. The analytical results obtained within the latest 2 years shows the following correlation as;

^{134}Cs/^{137}Cs =
$(0.070\pm0.001)\times\exp[(-0.000849\pm0.000007)\times T]$ (1),

where T means the time in days (T=0 is March 11, 2011). From Fig. 3 showing the time profile of ^{135}Cs/^{137}Cs isotopic ratio, we also obtained the following equation as;

^{135}Cs/^{137}Cs =
$(0.365\pm0.004)\times\exp[(0.000063\pm0.000005)\times T]$ (2).

From eqs. (1) and (2), the half-lives of ^{134}Cs and ^{137}Cs were evaluated as $T_{1/2(Cs\text{-}134)}$ = 2.08±0.02 y and $T_{1/2(Cs\text{-}137)}$ = 30.2±2.2 y respectively. We found that these values show the good relation with the literature data [6] (2.07 y for ^{134}Cs and 30.2 y for ^{137}Cs).

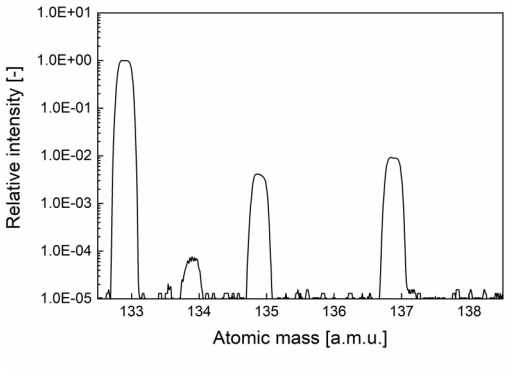

Fig. 1 Mass spectra of Cs recovered from environmental sample obtained at Fukushima prefecture observed at March 2019.

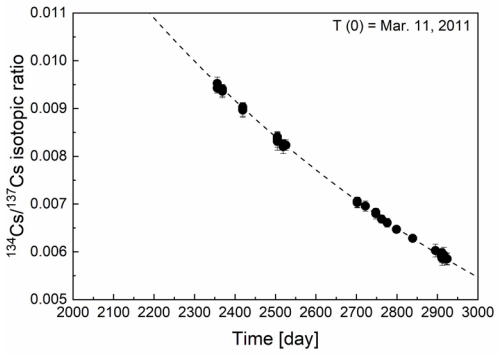

Fig. 2 Time profile of ^{134}Cs/^{137}Cs isotopic ratio. Broken line shows analysis results with equation of y=a×exp[b×x].

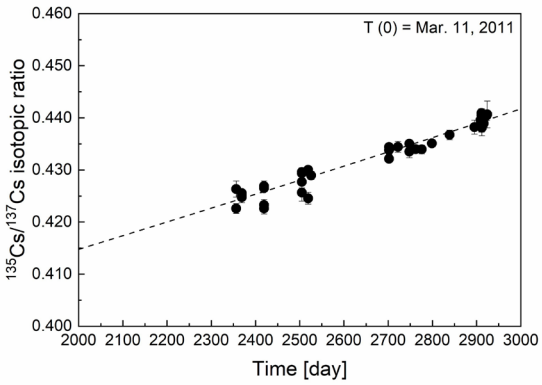

Fig. 3 Time profile of ^{135}Cs/^{137}Cs isotopic ratio. Broken line shows analysis results with equation of y'=a'×exp[b'×x].

[1] Y. Shibahara et al. KURRI progress report 2017,157.
[2] Y. Shibahara *et al.*, J. Nucl. Sci. Technol. 2014, 51, 575-579.
[3] Y. Shibahara *et al.,* Radiological issues for Fukushima's revitalized future. Springer. 2016. 33-46.
[4] Y. Shibahara *et al.,* J. Nucl. Sci. Technol. 2017, 54, 158-166.
[5] J. A. Dunne *et al.,* Talanta 2017, 174, 347-356.
[6] R.B. Firestone *et al.,* Table of Isotopes, John Wiley and Sons, New York, 1998.

PR10-5 EMF Mesurements of AgCl Concentration Cell in LiCl-KCl Eutectic Molten Salt Using Chloride Ion Conducting Solid Electrolyte

H. Sekimoto[1], Y. Saito[2] and N. Iwabuchi[1]

[1]*Department of Physical Science and Materials Engineering, Faculty of Science and Engineering, Iwate University*
[2]*Department of Materials Science and Engineering, Division of Science and Engineering, Graduate School of Arts and Science, Iwate University*

INTRODUCTION: Thermodynamic data of chemical species dissolved in molten salts such as activity, and activity coefficient are important to evaluate existing processes for treating nuclear materials. Such thermodynamic data are conventionally determined by measuring electromotive force using silver-silver chloride reference electrode. The electrodes are usually prepared by adding 1-5mol% of silver chloride into the same molten salt as sample and immersing silver wire. At the junction between sample and the electrode, porous ceramics or glass membrane are used. They can be used in limited system. In this study, a new type reference electrode was proposed. The proposed electrode consists of silver, pure silver chloride and anion conducting solid electrolyte. In this study, CaO doped LaOCl reported by Imanaka et al. [1] was employed as chloride ion conducting material.

EXPERIMENTS: CaO doped LaOCl is prepared by solid state reaction. The molar ratio of LaOCl : CaO was 85 : 15. The CaO doped LaOCl was attached on a side of cylindrical mullite tube with ceramic bond. Pure AgCl was inserted in the mullite tube with CaO doped LaOCl and heated at 600 °C to melt AgCl. Afterwards, silver wire was immersed in liquid AgCl. Subsequently, mullite tube with CaO doped LaOCl and silver wire immersed to construct the following AgCl concentration cell.

Ag(*s*) | AgCl(*l*, pure) (a_{AgCl} = 1) | LaOCl-CaO | AgCl (*l*, in LiCl-KCl eu.) (a_{AgCl} < 1) | Ag(*s*) (1)

The electromotive force of the cell (1) is evaluated as follows.

$$emf = -RT/F \ln a_{AgCl\ (l,\ in\ LiCl\text{-}KCl\ eu.)} \quad (2)$$

The addition of AgCl in LiCl-KCl eutectic molten salt and measurement of the *emf* was repeated several times.

RESULTS: As shown in Fig. 1, the relation between the *emf* and the concentration of AgCl in LiCl-KCl molten salt obeyed the Nernst equation. The activity of AgCl in LiCl-KCl eutectic molten salt was evaluated and shown in Fig. 2. The value obtained in this study well agree with the reported values [2-5].

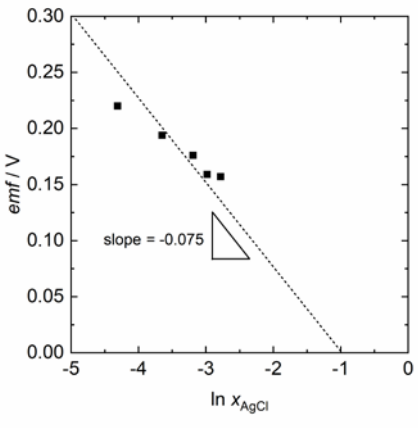

Fig. 1 Relation between the electromotive force of the AgCl concentration cell and the concentration of AgCl in LiCl-KCl eutectic molten salt.

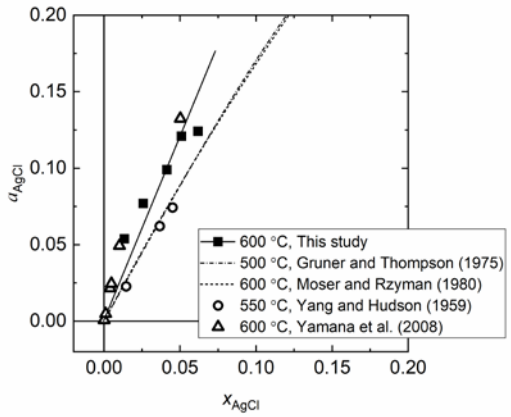

Fig. 2 Relation between the activity and the concentration of AgCl in LiCl-KCl eutectic molten salt.

REFERENCES:

[1] N. Imanaka, K. Okamoto and G. Adachi, Angew. Chem. Int. Ed., **41** (2002) 3890.
[2] O. Shirai, T. Nagai, A. Uehara and H. Yamana, J. Alloy. Compd., **456** (2008) 498.
[3] L. Yang and R. G. Hudson, J. Electrochem. Soc., **106** (1959) 986.
[4] A. C. Gruner and W. T. Thompson, Can. J. Chem., **53** (1975) 1084.
[5] Z. Moser and K. Ryzman, Electrochim. Acta, **25** (1980) 183.

Structural Change of Borosilicate Glass by Neutron Irradiation

T. Nagai, H. Kobayashi, Y. Okamoto, D. Akiyama[1], N. Sato[1], A. Uehara[2], T. Fujii[3], and S. Sekimoto[4]

Japan Atomic Energy Agency (JAEA)
[1]Institute of Multidisciplinary Research for Advanced Materials (IMRAM), Tohoku University
[2]National Institute of Quantum and Radiological Science and Technology (QST)
[3]Graduate school of Engineering, Osaka University
[4]Institute for Integrated Radiation and Nuclear Science, Kyoto University

INTRODUCTION: A high-level radioactive liquid waste from a reprocessing process for spent nuclear fuels is processed into a solidified waste made of a borosilicate glass. In our previous study, the structural change of neutron irradiated borosilicate glass was observed by using Raman spectrometry [1]. In this study, to understand this structural change by a neutron irradiation in detail, the irradiation test was carried out in 2017FY. The glass structure was estimated by using Raman spectrometry in 2018FY. As a mechanism of neutron irradiation on borosilicate glasses, the nuclear reaction $^{10}B(n,\alpha)^{7}Li$ was supposed, which was studied by S. Peuget, et al [2].

EXPERIMENTS: Two kinds of borosilicate glass of $17B_2O_3$-$65SiO_2$-$17Na_2O$-CeO_2-Y_2O_3 and $28B_2O_3$-$54SiO_2$-$17Na_2O$-CeO_2-Y_2O_3 were prepared based on the selection of chemical composition [3]. Raw material reagents of SiO_2, H_3BO_3, Na_2CO_3, CeO_2, and Y_2O_3 were loaded in an alumina crucible and were melted at 1,150°C in an electric furnace. After the molten glass samples were solidified by cooling to room temperature, they were cut into thin plates. In Dec. 2017, these thin plate samples were set in a polyethylene tube and were irradiated under the condition of 1,000 kW for 50 min in the Pn-2 of KUR. After the radioactivity of the samples reduced to the background level, the Raman spectra of the samples were measured by using a Raman spectrometer, NRS-3100 of JASCO.

RESULTS: As a structural change of borosilicate glass by the irradiation, an amount of Li would be increased by the $^{10}B(n,\alpha)^{7}Li$ reaction, and Li was expected to disconnect the Si-O bridging structure. So, the effect of the irradiation would be effectively evaluated by the Raman shifts of Si-O bridging structure. The Raman shifts of Si-O bridging structure of a borosilicate glass lies in the wavenumber of 850-1,250 cm^{-1}, and the peak positions of Raman shifts depend on the number of non-bridging oxygen, NBO. In this measurement, those Raman shifts were observed in 850-1,250 cm^{-1}, and the measured spectra was successfully separated into six Gaussian waves as shown in Fig. 1, where fitting error was negligible compared to the difference by irradiation. The Raman peak of Q^4 structure without NBO appeared in around 1,150 cm^{-1}, and those of Q^3, Q^2, and Q^1 structures with the NBO number = 1, 2, and 3 were in 1,090, 1,000, and 900 cm^{-1} respectively. The peaks of Q^2 and Q^3 structures can be subdivided into plural by the Si-O-X connecting state, and were divided into $Q^{2(1)}$, $Q^{2(2)}$, $Q^{3(1)}$, and $Q^{3(2)}$. Comparing the Raman shifts after irradiation with non-irradiation, it was observed that the peak heights of $Q^{2(1)}$, $Q^{2(2)}$, or $Q^{3(1)}$ decreased and that of Q^1 increased after the irradiation in Fig. 1. This result suggests that $Q^{2(1)}$, $Q^{2(2)}$, and $Q^{3(1)}$ structures change into Q^1 structure by the irradiation. In other words, it was considered that generated Li enters into a part of $Q^{2(1)}$, $Q^{2(2)}$, and $Q^{3(1)}$ structures easily.

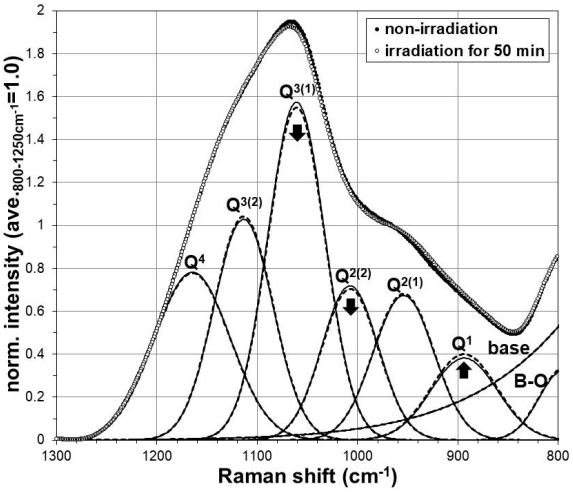

(1) $17B_2O_3$-$65SiO_2$-$17Na_2O$-CeO_2-Y_2O_3 sample.

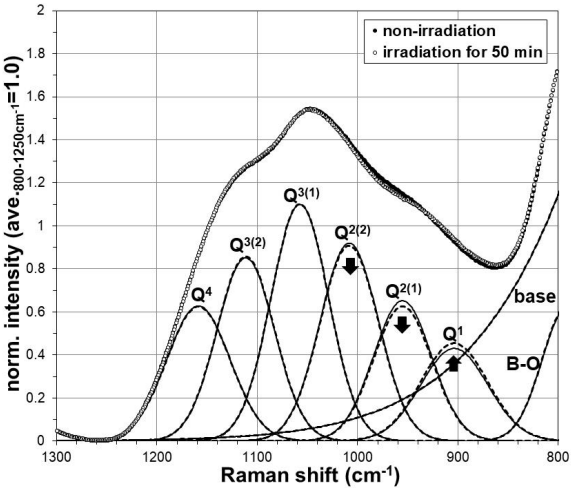

(2) $28B_2O_3$-54 SiO_2-$17Na_2O$-CeO_2-Y_2O_3 sample.

Fig. 1. Raman spectra and separated Gaussian waves. Open circles and dotted lines are after irradiation, and closed circles and fine lines are non-irradiation.

REFERENCES:

[1] T. Nagai, et al, 2014FY KURRI progress report, 26P11-4 (2015).
[2] S. Peuget, et al, Nucl. Inst. Methods in Phys. Res. B, **327** (2014) 22-28.
[3] T. Nagai, et al, 2017FY KURRI progress report, 29056 (2018).

PR10-7 Activation measurement for thermal-neutron capture cross-section of Cesium-135

S. Nakamura[1], A. Kimura[1], O. Iwamoto[1]
Y. Shibahara[2], A. Uehara[3], T. Fujii[4],

[1]*Japan Atomic Energy Agency*
[2]*Institute for Integrated Radiation and Nuclear Science, Kyoto University*
[3]*National Institutes for Quantum and Radiological Science and Technology*
[4]*Graduate School of Engineering, Osaka University*

INTRODUCTION: In recent years, transmutation researches have been reconsidered. The "ImPACT" project [1] is one of such research trends. In this project, following LLFP nuclides are listed to be transmuted: ^{107}Pd, ^{93}Zr, ^{135}Cs, and ^{79}Se. When considering nuclear transmutation of these LLFPs by using neutrons, accurate data of neutron capture cross-sections are required to evaluate the transmutation and/or reaction rate. Two nuclides of ^{107}Pd and ^{93}Zr have been previously measured at J-PARC [2,3]. On the other hand, it is very difficult to obtain ^{135}Cs and ^{79}Se samples for measurements. This is the reason why there are a few ^{135}Cs data and no ^{79}Se data. The authors chose ^{135}Cs for measurements because we got an idea of using ^{135}Cs contained as an impurity in a ^{137}Cs standard solution.
This work is aimed to measure the thermal-neutron cross-section of the ^{135}Cs (n, γ) ^{136}Cs reaction.

EXPERIMENTS: A standard solution of ^{137}Cs was obtained through the Japan Radioisotope Association. The isotope ratio of ^{135}Cs and ^{137}Cs was determined by mass spectrometry. The mass spectrometer TRITON (Thermo Fisher Scientific, Inc.) was used for this analysis. A small amount (about 10 Bq) of the ^{137}Cs solution was pipetted onto a Re filament together with a TaO activator, and then the filament was dried. The loaded filament was attached onto the ion source of the spectrometer. From mass yields of Cs isotopes in the mass spectrum, the ratio of ^{135}Cs and ^{137}Cs was found to be 0.868±0.004 (±2σ).

A small amount of 1 kBq solution was taken from the same ^{137}Cs standard solution, and then dropped onto a 5-mm-square chemical filter. The ^{137}Cs loaded filters were dried by an infrared lamp. The filter was wrapped with high purity aluminum foil together with pieces of Au/Al and Co/Al alloy wires to monitor neutron flux components at an irradiation position. The ^{137}Cs loaded filter with the monitor set was used as an irradiation target (called "a bare target"). The same ^{137}Cs loaded filter and monitor set were sandwiched both sides with a Gadolinium (Gd) foil of 10 mm×15 mm×25 μm^t in size (called "a Gd filtered target") to estimate contributions by epi-thermal neutrons. The irradiations of the targets were performed at the Hydraulic tube of the Kyoto University Reactor (KUR) in 5-MW power operation. The bare target was irradiated for 3 hours, and the Gd filtered one for 6 hours. The γ-ray measurements were performed later from the end of the irradiation. A high-purity Ge detector was used to measure the γ rays emitted from Cs isotopes to obtain their induced activities. **Figure 1** shows an example of γ-ray spectrum of the Gd filtered target. Decay γ rays emitted from ^{137}Cs and ^{136}Cs were clearly observed at the γ-ray energies of 662 keV and 819 keV. Sufficient statistics for the γ-ray peaks were obtained. Since the ratio of ^{135}Cs and ^{137}Cs have been determined in advance, the yield of 662-keV γ ray can give an amount of ^{135}Cs in the target.

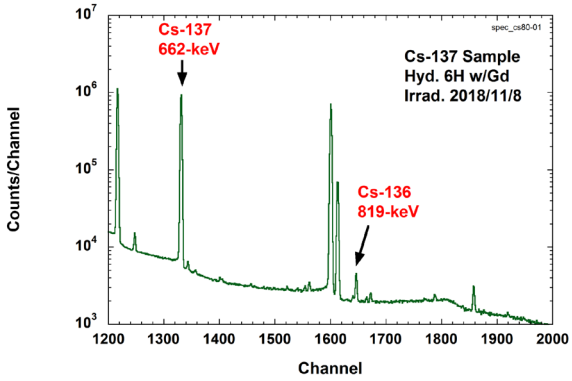

Fig.1 Gamma-ray spectrum of Gd filtered ^{137}Cs target irradiated by reactor neutrons at KUR

Then, the ^{135}Cs(n,γ)^{136}Cs reaction rate can be obtained from the yield of 819-keV γ ray due to ^{136}Cs. The reaction rates in the cases of bare and Gd-filtered targets were determined, and the thermal-neutron capture cross-section can be derived by the analysis based on Westcott's convention [4]. The present result is consistent with the past reported value [5] within the limits of errors. Further analysis is now in progress.

Acknowledgement

The authors would like to appreciate staffs of Kyoto University Research Reactor Institute for their support. This research was funded by ImPACT Program of Council for Science, Technology and Innovation (Cabinet Office, Government of Japan).

REFERENCES:

[1] http://www.jst.go.jp/impact/index.html
[2] S. Nakamura *et al.*, Nuclear Data Sheets, 2014;**119**:143.
[3] J. Hori *et al.*, AESJ fall meeting, 2010.
[4] C.H. Westcott *et al.*, "*Proc.2nd Int.Conf.Peaceful Use of Atomic Energy, Geneva*", 1958;**16**:70.
[5] T. Katoh *et al.*, J.Nucl.Sci.Technol., 1997; **34**: 431.

PR10-8 Exchange Reaction of Proton in Hydroxide with Tritium in Aqueous Solution

H. Hashizume, A. Uehara[1], S. Fukutani[2], K. Fujii, T. Ando

National Institute for Materials Science
[1]National Institute for Quantum and Radiological Science and Technology
[2]Institute for Integrated Radiation and Nuclear Science, Kyoto University

INTRODUCTION: Tritium (T) is one of radioactive elements. Since the characteristics are almost the same as hydrogen (H), it is very difficult to separate tritium from water. We have a large amount of radioactively contaminated water for the Fukushima Daiich Nuclear Power Station Accident. Because HTO is included in the radioactively contaminated water, it can not be discarded and is increasing. For the removal of HTO from water, Koyanaka and Miyatake (2015) reported that about 30% amounts of tritium in water including tritium was caught by manganese oxide for about 20 min [1]. Hashizume et al. (2016) investigated that tritium was discriminated in the formation of a hydroxide from an oxide in water including tritium [2]. They also examined the ion exchange between proton in hydroxide and tritium in water [3]. A few % of tritium was removed in water including T by those treatments.

We investigate the change of the ion exchange between tritium in water and proton in a hydroxide to the different concentration of tritium in water, and show the isotherm for the ion exchange between tritium and proton to the concentration of tritium in water by the hydroxide.

EXPERIMENTS: We used water including tritium which was prepared in Institute for Integrated Radiation and Nuclear Science, Kyoto University. Magnesium hydroxide ($Mg(OH)_2$) and calcium hydroxide ($Ca(OH)_2$) were used as the ion exchange materials. Water including tritium was diluted by deionized water, properly. For the ion exchange, 1g of the ion exchange material and 8 cm^3 of diluted water were put in the glass bottle with stopper. The suspension was shaken for 5 hours by the rotary shaker. Hashizume et al. (2018) showed that 5 hours were enough time to achieve the equilibrium of the ion exchange [4]. After shaking, the suspension was centrifuged and supernatant was filtered by 0.45 or 0.2 μm of a filter. For the measurement by a scintillation detector (Packard, Liquid Scintillation Analyzer), 1 cm^3 of the supernatant or the original water including tritium and 20 $cm^3$of the liquid scintillator were pour into the glass vial.

The extent of the ion exchange was estimated by the following equation.

$$E=(C_0-C)\bullet V/W \quad (1)$$

where E is the extent of ion exchange, C_0 is the concentration of tritium in water, C is the concentration of tritium in supernatant, V is the volume of added water and W is the weight of the ion exchange material.

RESULTS: The isotherms for the ion exchange by $Mg(OH)_2$ and $Ca(OH)_2$ are shown in Fig. 1. The extent of the ion exchange by $Mg(OH)_2$ was higher than that by $Ca(OH)_2$. The isotherms were adopted to Langmuir and Freundlich equation. The Langmuir and Freundlich equation are

Langmuir equation: $E=a\bullet E_s\bullet B/(1+a\bullet B)$ (2)

Freundlich equation: $E= K_f\bullet B^{1/n}$ (3)

where E_s is the saturated ion exchange capacity, B is equilibrium concentration, a, K_f and n are constant.

The parameters of Langmuir and Freunlich equations are shown in Table 1. And the isotherms from Langmuir and Freundlich equations are also shown in Fig. 1. The Freundlich equation might be more fitted than the Langmuir equation.

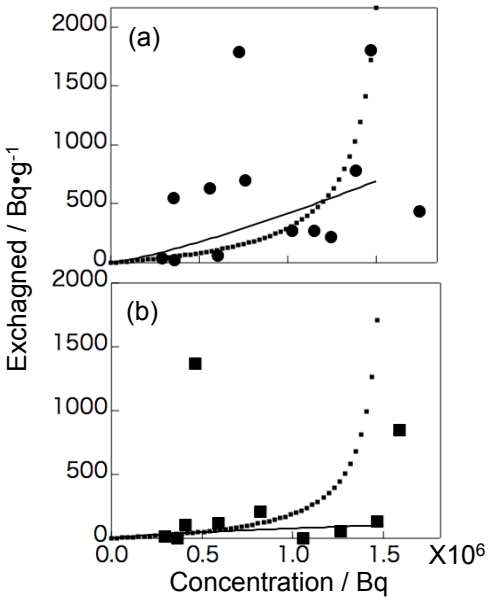

Fig.1 Isotherms for ion exchange of tritium by $Mg(OH)_2$ (a) and $Ca(OH)_2$ (b). The dot and black lines are for Langmuir and Freundlich equation, respectively.

Table 1 Parameters of Langmuir and Freundlich equation.

	Langmuir			Freundlich	
	$Mg(OH)_2$	$Ca(OH)_2$		$Mg(OH)_2$	$Ca(OH)_2$
a	-6.1x10-7	-6.4x10-7	K_f	1.37	0.0033
E_s	-185.2	-106.4	1/n	1.24	0.723

REFERENCES:

[1] H.Koyanaka & H. Miyatake, *Separation Science Technology*, **50** (2015) 2142-2145.
[2] H.Hashizume *et al.,* Tokugann 2016-135839 (2016) (Japanese patent in Japanese).
[3]H.Hashizume *et al.*, Tokugann 2018-43792 (2018) (Japanese patent in Japanese).
[4] H.Hashizume *et al.*, KURRI Progress Report (2017) C05-6.

PR10-9 Solvent Extraction Behavior of Fission Product Elements

Y. Araki[1], M. Morita[1], T. Kawakami[1], C. Kato[1], A. Uehara[2], S. Fukutani[2] and T. Fujii[1]

Graduate School of Engineering, Osaka University
[2]KURNS, Kyoto University

INTRODUCTION: By separating the long lived nuclides from high-level radioactive waste, it is possible to significantly reduce the potential hazard of waste, thereby reducing long-term risk. Palladium (Pd) is a fission product element contained in the spent fuel. The half-life of ^{107}Pd is 6.5×10^6 years, and is subjected to separation. Also, Pd has a large cross section area to the fast neutron, so it is likely to interfere with fission of minor actinides (MA). In this study, we focused on the separation of Pd and studied the solvent extraction behavior of Pd from a nitric acid solution. Furthermore, we compared with nickel (Ni) which is the same group element as Pd for better understanding.

EXPERIMENTS: Palladium and Ni were prepared in nitric acid as the aqueous phase. For the organic phase, tetradodecyl diglycolamide (TDdDGA), N,N,N',N',N",N"-hexaoctylnitriloacetamide (HONTA) and alkyldiamideamine (ADAAM) was prepared in dodecane. HONTA and ADAAM are novel extractants developed by Japan Atomic Energy Agency (JAEA) [1]. After the two phases were stirred for 30 minutes, phase separation was performed by centrifugation. The back extraction was performed using the phase-separated organic phase and diluted nitric acid, which was then separated by centrifugation. The element concentration was measured in the aqueous phase after the fore extraction and back extraction using inductively coupled plasma－atomic emission spectrometry (ICP-AES), and the distribution ratio was determined.

RESULTS and DISCUSSION: The distribution ratio of Pd and Ni and its dependency of nitric acid concentration is shown in figure 1. For Pd, when using the novel extractants, the distribution ratio peaked at a nitric acid concentration around 0.2 M. In addition, it was found that the distribution ratio was up to 103 times higher than using TDdDGA in the high acidity region. For Ni, it was found that the distribution ratio was generally low for all extractants.

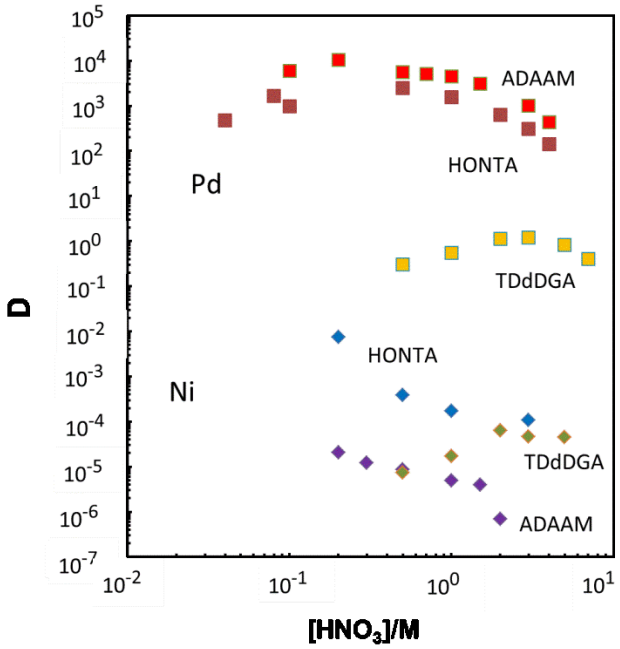

Fig. 1. Distribution ratio of Pd and Ni and its dependency on nitric acid concentration.

REFERENCES:

[1] H. Suzuki *et. al.,* Anal. Sci., **32** (2016) 477-479.

PR10-10 Electrochemical behavior of zirconium in molten lithium – calcium chloride to develop processing nuclear fuel debris

T. Nagasawa, T. Emori[1], H. Matsuura[1,2], A. Uehara[3]

Faculty of Engineering, Tokyo City University, Japan
[1]Graduate School of Engineering, Tokyo City University, Japan
[2]Atomic Energy Research Laboratory, Tokyo City University, Japan
[3]National Institutes for Quantum and Radiological Science and Technology, Japan

INTRODUCTION: In order to develop processing nuclear fuel debris caused by nuclear accident of the Fukushima Daiichi Nuclear Power Plant following from huge earthquake and tsunami on 2011, we have proposed selective fluorination and molten salt electrolysis to separate uranium from nuclear fuel debris. Process concept is as follows; 1) selective fluorination; UO_2 was fluorinated in nuclear fuel debris using HF gas[1], 2) selective dissolution; UF_4 was dissolved in molten salt and 3) molten salt electrolysis; uranium ions were reduced in molten salt, and uranium metal or oxide was deposited on electrode. However coexisting zirconium can be also fluorinated with uranium and zirconium oxide will be remaining at the upstream process. Therefore, electroreduction of uranium cannot be made because standard redox potential of zirconium is more positive than that of uranium. Zirconium electrochemistry due to the presence fluoride and oxide ions should be investigated to reduce zirconium concentration in molten bath. In this year, we choose molten LiCl-$CaCl_2$ for electrolysis bath since no cationic species are disturb at uranium electro-reduction even in co-existence of fluoride anion.

EXPERIMENTS: All the electrochemical measurements using molten LiCl-$CaCl_2$ have been performed in an electric furnace which is built inside a glove box filled with dried argon atmosphere using an electrochemical analyzer. Electrochemical analysis has been performed as both cyclic voltammetry and linear sweep voltammetry by using the electrodes as follows: working electrode: molybdenum, counter electrode: pyrographite and reference electrode: silver wire dipped in molten LiCl-KCl + AgCl inside the borosilicate tube. Aluminium oxide ceramics was used as a crucible, and temperature condition is at 700 ^{o}C. To observe the fluoride addition effect, both zirconium chloride and fluoride were used as a zirconium solute (1 wt%) by addition to the pre-mixed LiCl-$CaCl_2$ electrolysis bath. Duration of pre-reduction before linear sweep voltammetry is 1 minute.

RESULTS AND DISCUSSION: Before going to simulant of fluorinated fuel debris, electrochemical behavior of zirconium in molten LiCl- $CaCl_2$ without fluoride have been performed. In cyclic voltammogram, both 2 steps redox couples (Zr(VI)/Zr(II) and Zr(II)/Zr(0)) were identified. However, as comparison to previously obtained data which was performed by using molten LiCl-KCl eutectic as electrolysis bath, zirconium redox potential related to metal was significantly shifted to positive value. Next, cyclic voltammetry of LiCl-$CaCl_2$-ZrF_4(1wt%) has been also performed. Redox couple of Zr(IV)/Zr(II) was observed at R: -0.77 V and O:-0.18 V and that of Zr(II)/Zr(0) was at R:-0.90 V and O:-0.83 V. Also in this case, zirconium reduction peak was significantly positive shifted from that in molten LiCl-KCl bath and the value of potential was very close to that in LiCl-$CaCl_2$-$ZrCl_4$. With increasing cathodic sweep limit of potential, current density increased rapidly, thus zirconium would be electroreduced with calcium though further characterization of electrodeposit will be necessary. Exactly using the same sample of molten LiCl-$CaCl_2$-ZrF_4(1wt%), linear sweep voltammetry has been applied, which is shown in Fig. 1. In the case of pre-reduction at more negative potential than -0.90V, huge 2 oxidative peaks has been appeared between -0.70 V and -0.60 V. While in the case of pre-reduction at less negative potential than -0.85 V, these huge peak was completely dissapeared. Therefore, by using LiCl-$CaCl_2$ electrolysis bath, co-reduction of zirconium and calcium is unavoidable.

From these results, we can suggest the process design for fuel debris treatment is as follows. 1) As shown in increase of current density using zirconium fluoride as solute, once fluorinated fuel debris will be compatible to molten chloride bath, since $ZrCl_4$ has high vapor pressure. 2) As comparison with the case of molten LiCl-KCl, electroreduction potential of zirconium is positively shifted in molten LiCl-$CaCl_2$. It seems great advantage of electrodeposition but more important factor is how to separate uranium and zirconium. We have also noticed on the local structural variation in each case, so further systematic investigation of related material will be required in order to suggest much concrete process design for treatment of fuel debris. .

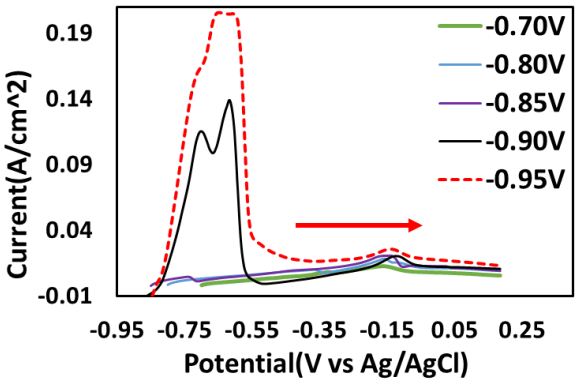

Fig.1 LSV at molten LiCl-$CaCl_2$ containing 1 wt% of ZrF_4.

REFERENCE:

[1]T. Ono, N. Sato, A. Nezu, T. Uchiyama, H. Matuura, *ECS,Tr ans.*,**75** (2016) 87.